

# Supplementary Material

## **Predicted Optimal Bifunctional Electrocatalysts for the Hydrogen Evolution Reaction and the Oxygen Evolution Reaction Using Chalcogenide Heterostructures Based on Machine Learning Analysis of in Silico Quantum Mechanics Based High Throughput Screening**

*Lei Ge,<sup>1+</sup> Hao Yuan,<sup>1+</sup> Yuxiang Min,<sup>1</sup> Li Li,<sup>1</sup> Shiqian Chen,<sup>1</sup>*

*Lai Xu<sup>\*</sup>,<sup>1</sup> and William A. Goddard III<sup>\*2</sup>*

1 Institute of Functional Nano & Soft Materials (FUNSOM), Jiangsu Key Laboratory for Carbon-Based Functional Materials & Devices, Soochow University, Suzhou 215123, China

2 Materials and Process Simulation Center (MSC) and Joint Center for Artificial Photosynthesis (JCAP), California Institute of Technology, Pasadena, CA 91125

<sup>+</sup> Contributed equally to this work

<sup>\*</sup>To whom correspondence should be addressed.

E-mail: xulai15@suda.edu.cn, wag@caltech.edu

## Calculation method of HER and OER activity

**$\Delta G$  for Hydrogen Evolution Reaction:** the  $\Delta G$  for each step under  $U=0$  ( $\text{pH}=0$  and  $T=298.15$  K).



$$\Delta E_{*H} = \frac{1}{n}(E(*+nH) - E_* - \frac{n}{2}E_{H_2}) \quad (\text{S2})$$

$$\begin{aligned} \Delta G_{*H} &= \Delta G(H^+ + e^- + * \leftrightarrow *H) = \mu_{*H} - \mu_{H^+} - \mu_{e^-} - \mu_* = \mu_{H^*} - \frac{1}{2}\mu_{H_2} - \mu_* \\ &= \left(E_{*H} - \frac{1}{2}E_{H_2} - E_*\right) + \left(E_{\text{ZPE}(*H)} - \frac{1}{2}E_{\text{ZPE}(H_2)} - E_{\text{ZPE}(*)}\right) - T \times \left(S_{*H} - \frac{1}{2}S_{H_2} - S_*\right) \quad (\text{S3})^1 \end{aligned}$$

**$\Delta G$  for Oxygen Evolution Reaction:** the  $\Delta G$  for each step under  $U=0$  ( $\text{pH}=0$  and  $T=298.15$  K).

$$\Delta E_{*OH} = E_{*OH} - E_* - \left(E_{H_2O} - \frac{1}{2}E_{H_2}\right) \quad (\text{S4})$$

$$\Delta E_{*OOH} = E_{*OOH} - E_* - \left(2 \times E_{H_2O} - \frac{3}{2}E_{H_2}\right) \quad (\text{S5})$$

$$\Delta E_{*O} = E_{*O} - E_* - \left(E_{H_2O} - E_{H_2}\right) \quad (\text{S6})^2$$

$$\begin{aligned} \Delta G_{*O} &= \Delta G(H_2O(g) + * \rightarrow *O + H_2(g)) = \mu_{*O} + \mu_{H_2} - \mu_{H_2O} - \mu_* \\ &= \left(E_{*O} + E_{H_2} - E_{H_2O} - E_*\right) + \left(E_{\text{ZPE}(*O)} + E_{\text{ZPE}(H_2)} - E_{\text{ZPE}(H_2O)} - E_{\text{ZPE}(*)}\right) - \\ &\quad T \times (S_{*O} + S_{H_2} - S_{H_2O} - S_*) \quad (\text{S7})^3 \end{aligned}$$

$$\begin{aligned} \Delta G_{*OH} &= \Delta G\left(H_2O(g) + * \rightarrow *OH + \frac{1}{2}H_2(g)\right) = \mu_{*OH} + \frac{1}{2}\mu_{H_2} - \mu_{H_2O} - \mu_* \\ &= \left(E_{*OH} + \frac{1}{2}E_{H_2} - E_{H_2O} - E_*\right) + \left(E_{\text{ZPE}(*OH)} + \frac{1}{2}E_{\text{ZPE}(H_2)} - E_{\text{ZPE}(H_2O)} - E_{\text{ZPE}(*)}\right) - \\ &\quad T \times \left(S_{*OH} + \frac{1}{2}S_{H_2} - S_{H_2O} - S_*\right) \quad (\text{S8})^4 \end{aligned}$$

$$\begin{aligned} \Delta G_{*OOH} &= \Delta G\left(2H_2O(g) + * \rightarrow *OOH + \frac{3}{2}H_2(g)\right) = \mu_{*OOH} + \frac{3}{2}\mu_{H_2} - 2\mu_{H_2O} - \mu_* \\ &= \left(E_{*OOH} + \frac{3}{2}E_{H_2} - 2E_{H_2O} - E_*\right) + \left(E_{\text{ZPE}(*OOH)} + \frac{3}{2}E_{\text{ZPE}(H_2)} - 2E_{\text{ZPE}(H_2O)} - \right. \\ &\quad \left. E_{\text{ZPE}(*)}\right) - T \times \left(S_{*OOH} + \frac{3}{2}S_{H_2} - 2S_{H_2O} - S_*\right) \quad (\text{S9})^5 \end{aligned}$$

**The  $\Delta G$  for each step can be calculated by:**



$$\Delta G_1 = \mu_{* \text{OH}} + \mu_{\text{H}^+} + \mu_{\text{e}^-} - \mu_{\text{H}_2\text{O}} - \mu_* = \mu_{* \text{OH}} + \frac{1}{2} \mu_{\text{H}_2} - \mu_{\text{H}_2\text{O}} - \mu_* = \Delta G_{* \text{OH}} \quad (\text{S11})$$



$$\Delta G_2 = \mu_{* \text{O}} + \mu_{\text{H}^+} + \mu_{\text{e}^-} - \mu_{* \text{OH}} = \mu_{* \text{O}} + \frac{1}{2} \mu_{\text{H}_2} - \mu_{* \text{OH}} = \Delta G_{* \text{O}} - \Delta G_{* \text{OH}} \quad (\text{S13})$$



$$\Delta G_3 = \mu_{* \text{OOH}} + \mu_{\text{H}^+} + \mu_{\text{e}^-} - \mu_{* \text{O}} - \mu_{\text{H}_2\text{O}} = \mu_{* \text{OOH}} + \frac{1}{2} \mu_{\text{H}_2} - \mu_{* \text{O}} - \mu_{\text{H}_2\text{O}} = \Delta G_{* \text{OOH}} - \Delta G_{* \text{O}} \quad (\text{S15})$$



$$\Delta G_4 = \mu_* + \mu_{\text{O}_2} + \mu_{\text{H}^+} + \mu_{\text{e}^-} - \mu_{* \text{OOH}} = \mu_* + \mu_{\text{O}_2} + \frac{1}{2} \mu_{\text{H}_2} - \mu_{* \text{OOH}} = 4.92 - \Delta G_{* \text{OOH}} \quad (\text{S17})$$

**Calculation of OER Overpotential:** The theoretical overpotential  $\eta$ , which is determined by the potential limiting step:

$$\eta = \max [ \Delta G_1, \Delta G_2, \Delta G_3, \Delta G_4 ] / e - 1.23[\text{V}] \quad (\text{S18})^6$$

## Supplementary Figures

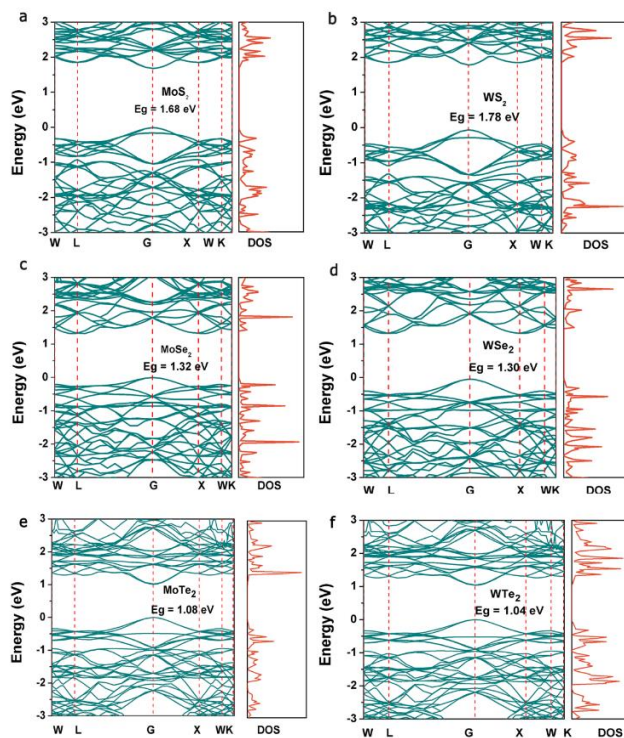


**Figure S1.** Band structures and density of states of the single-layer  $\text{MoS}_2$ ,  $\text{WS}_2$ ,  $\text{WSe}_2$ ,  $\text{MoSe}_2$ ,  $\text{MoTe}_2$  and  $\text{WTe}_2$  (a, b, c, d, e, f), computed at the level of PBE+U respectively.

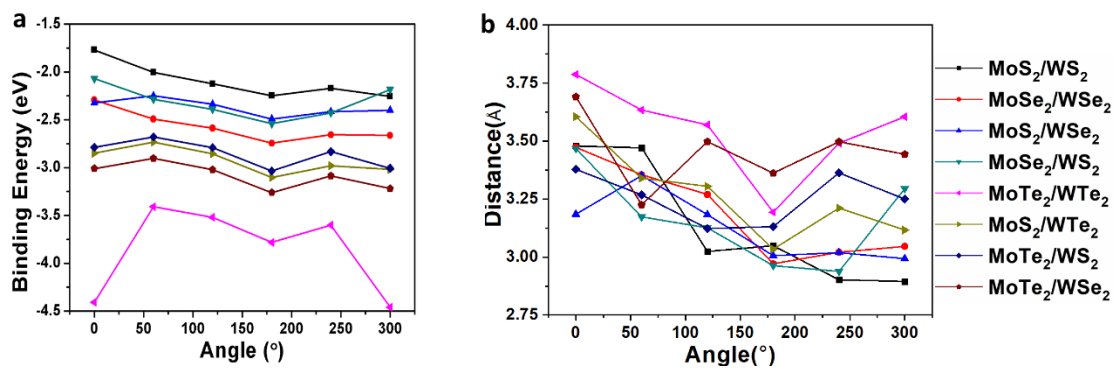


**Figure S2.** The trend of binding energy and distance for various heterojunctions with various angles.

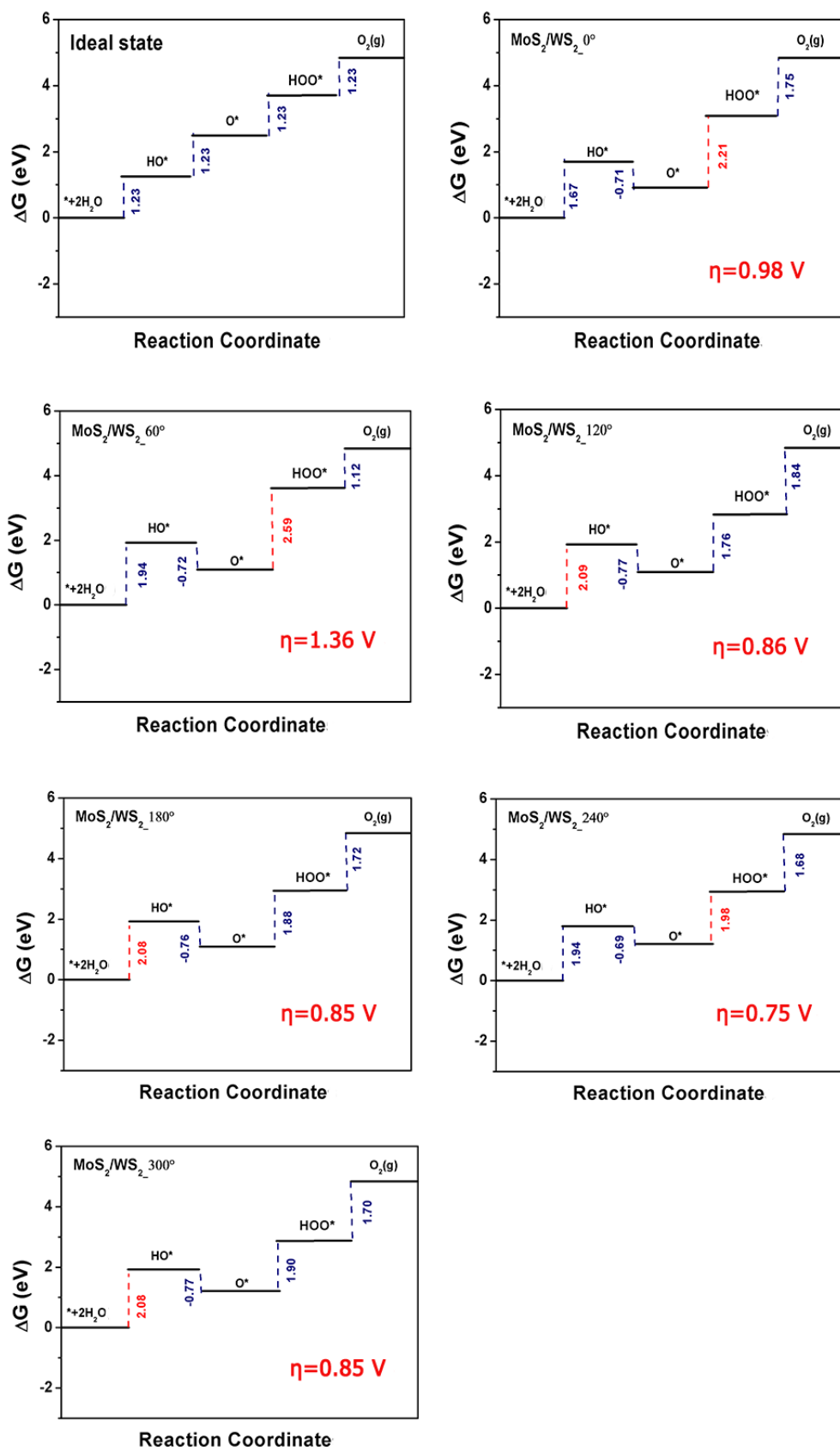
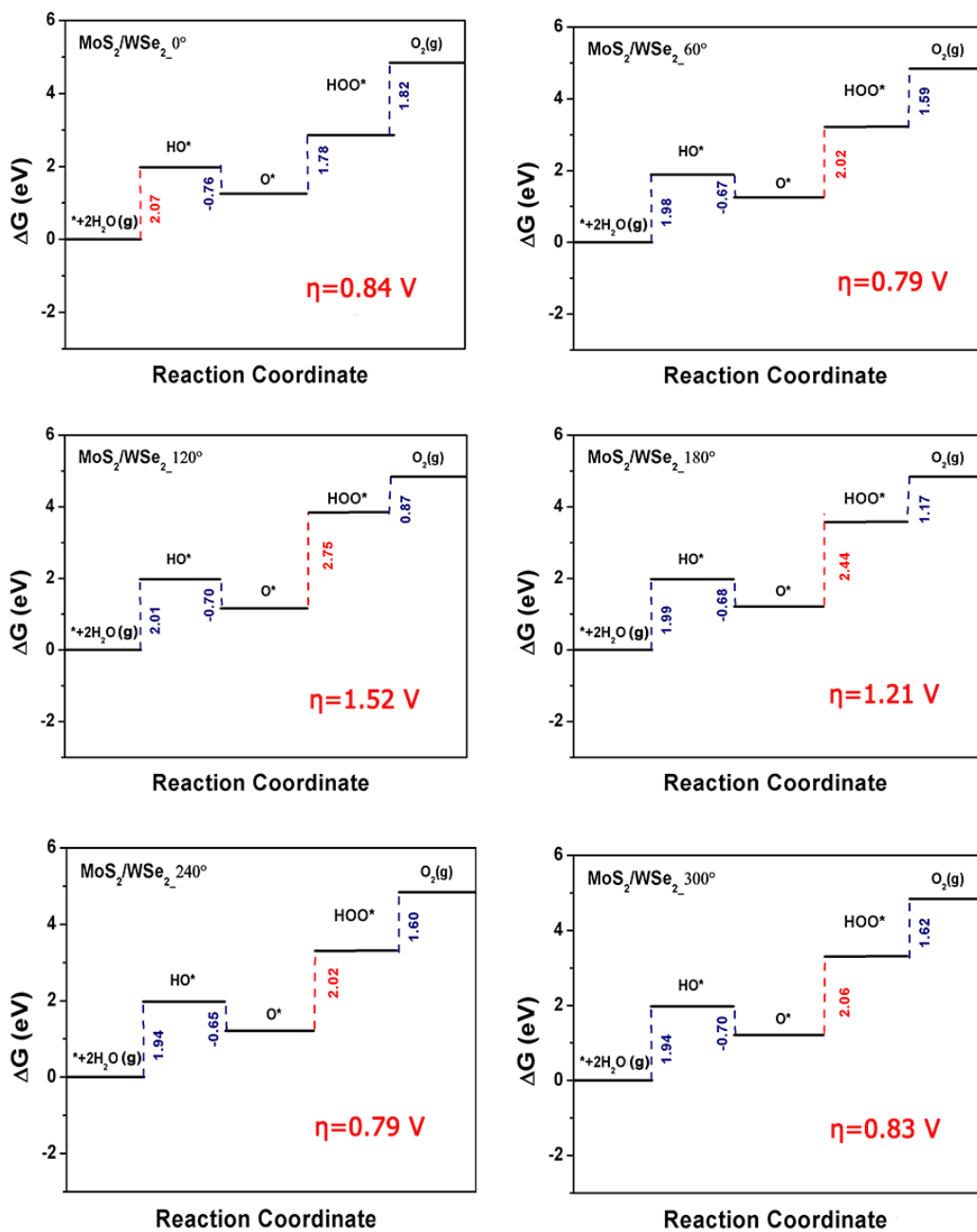
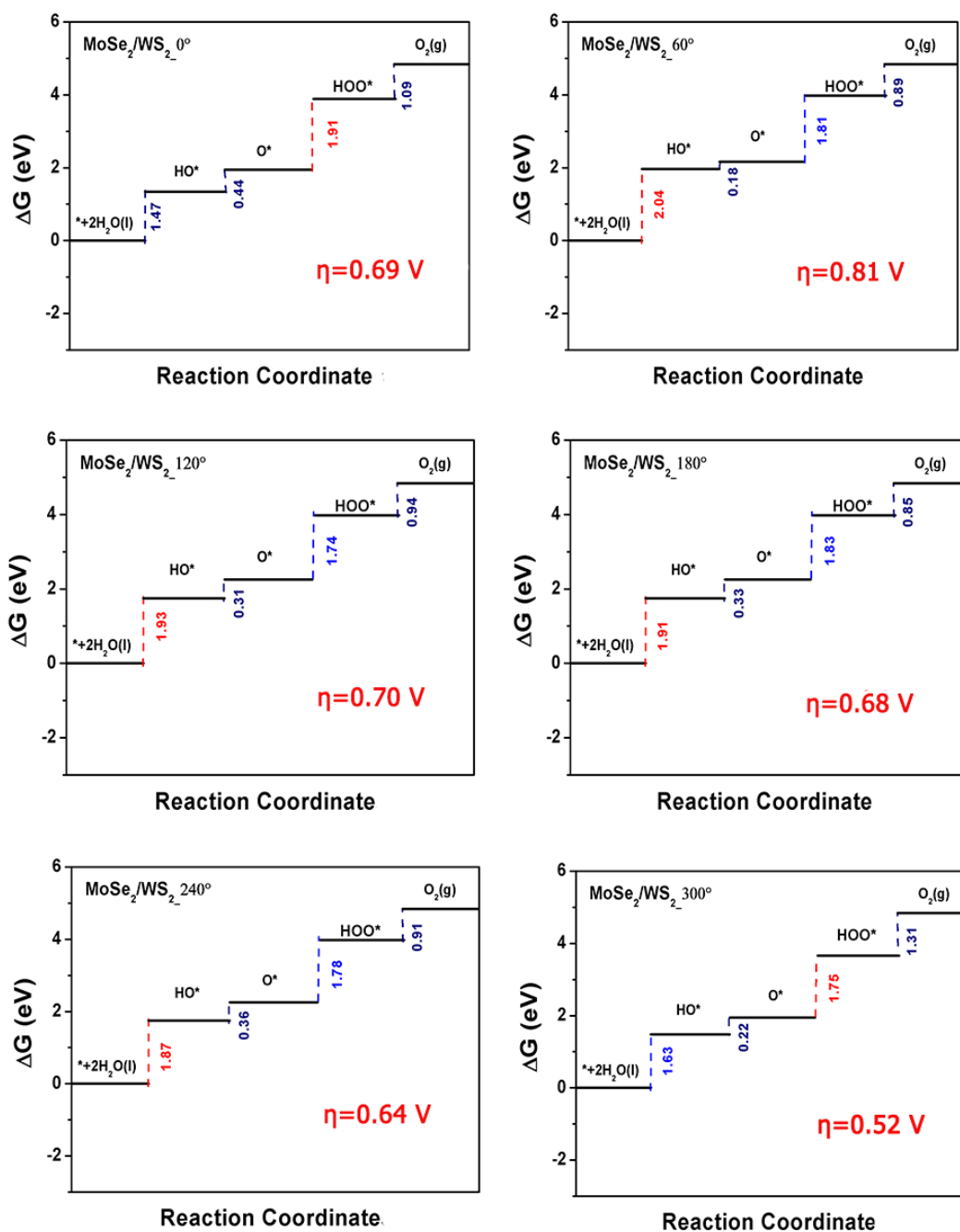


Figure S3. Free-energy diagram for OER of MoS<sub>2</sub>/WS<sub>2</sub> at zero electrode potential.



**Figure S4.** Free-energy diagram for OER of MoS<sub>2</sub> supported on WSe<sub>2</sub> at zero electrode potential.



**Figure S5.** Free-energy diagram for OER of MoSe<sub>2</sub>/WS<sub>2</sub> at zero electrode potential.

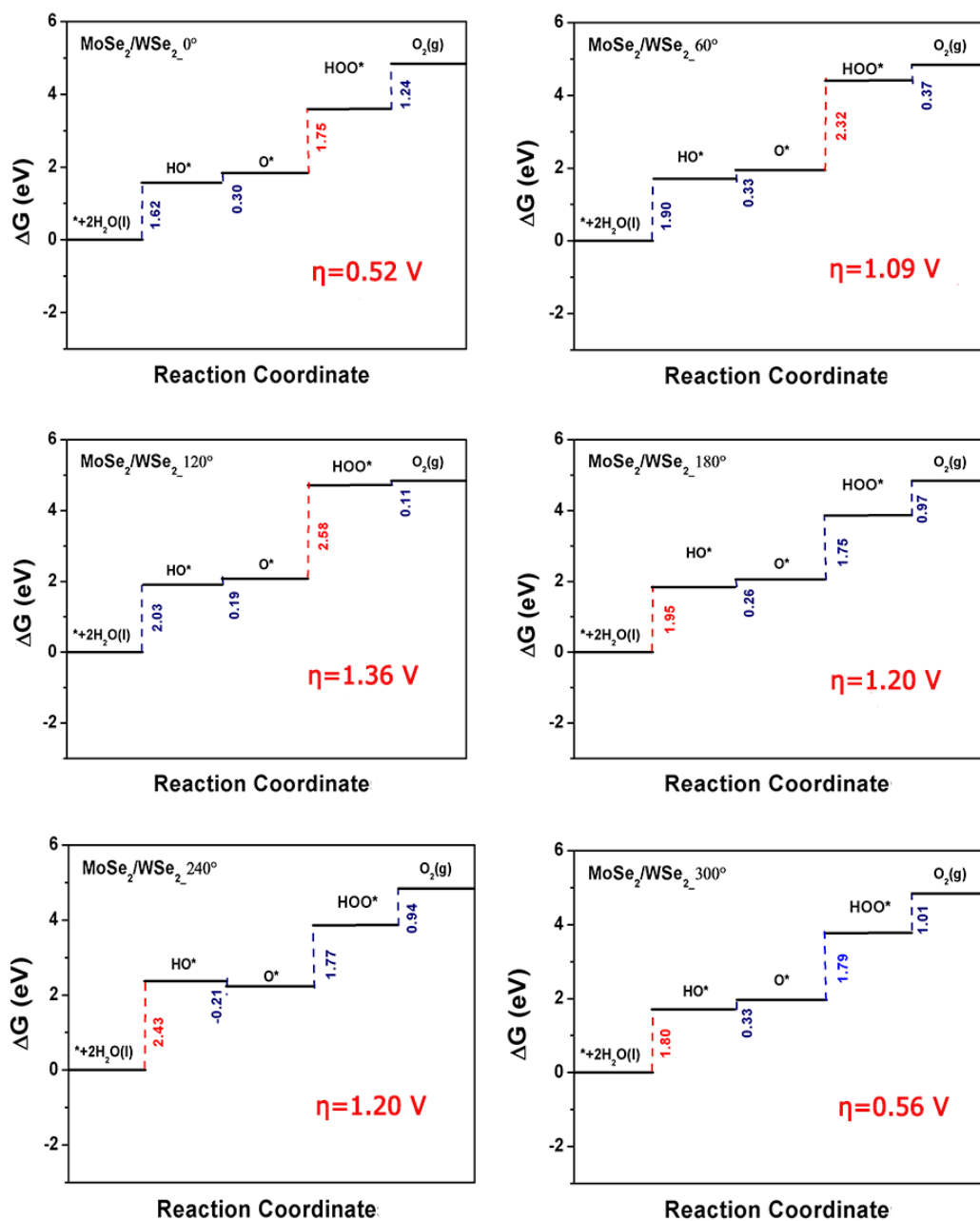


**Figure S6.** Free-energy diagram for OER of MoSe<sub>2</sub>/WSe<sub>2</sub> at zero electrode potential.

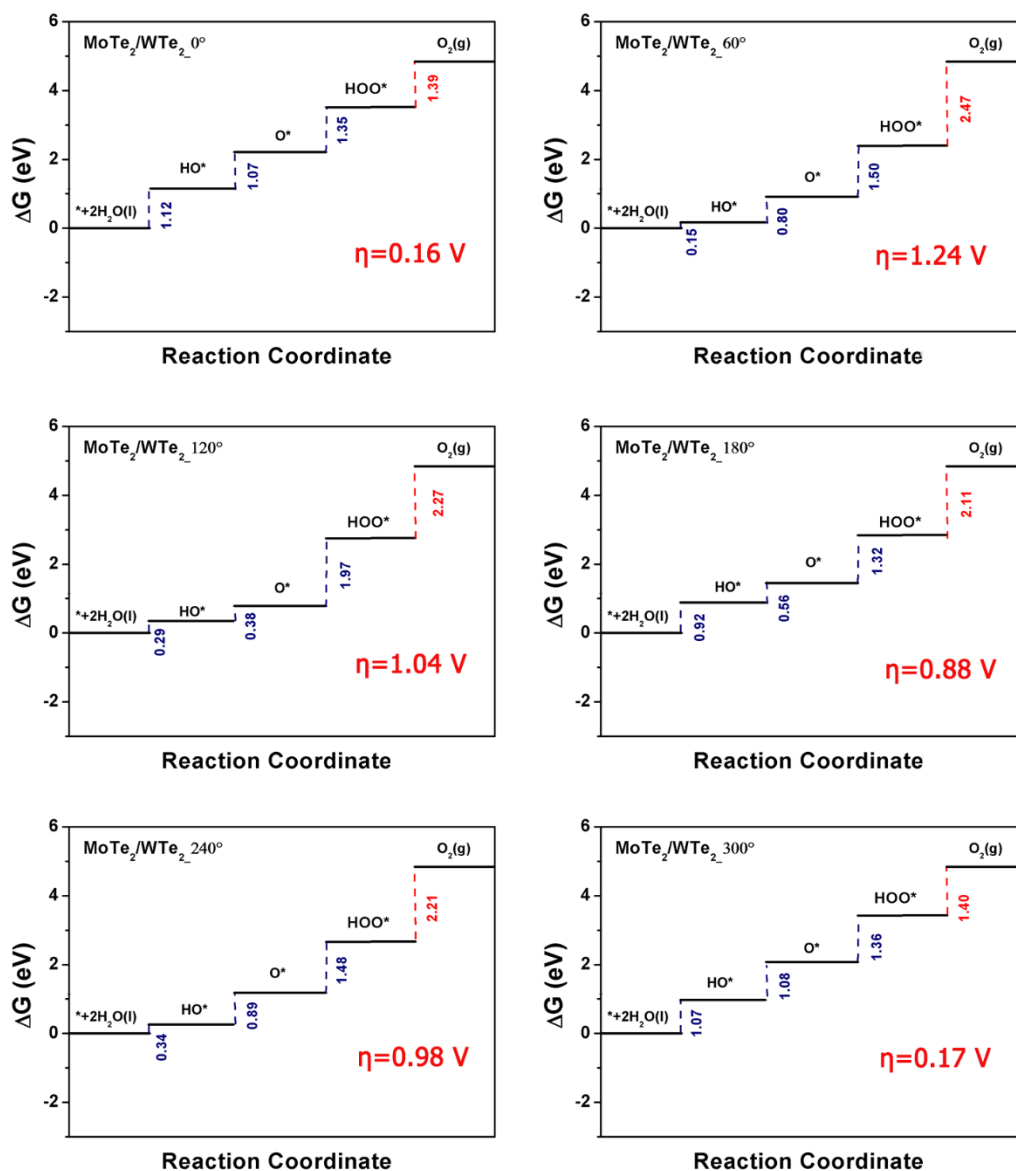


**Figure S7.** Free-energy diagram for OER of MoTe<sub>2</sub>/WTe<sub>2</sub> at zero electrode potential.

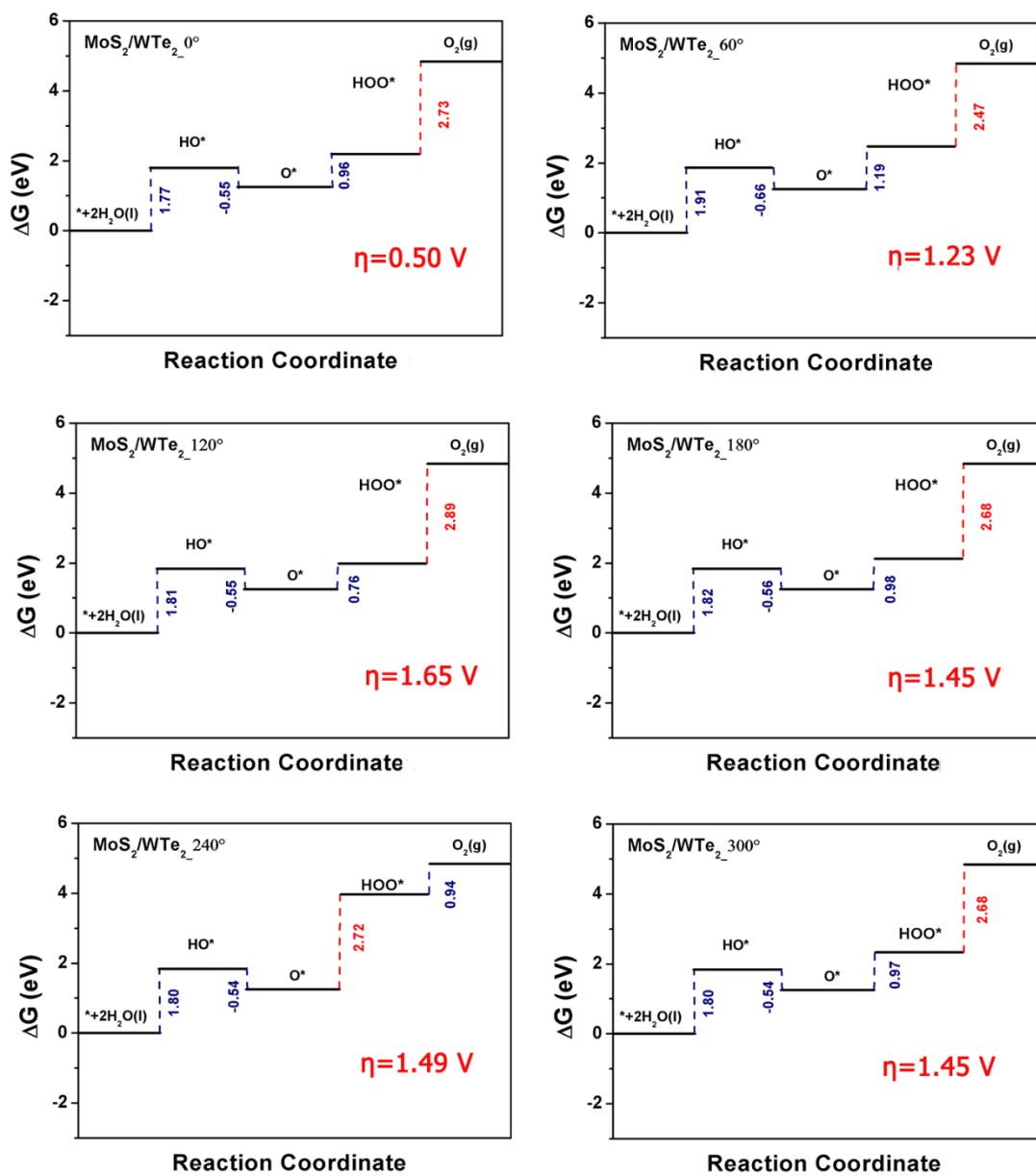


**Figure S8.** Free-energy diagram for OER of MoS<sub>2</sub>/WTe<sub>2</sub> at zero electrode potential.

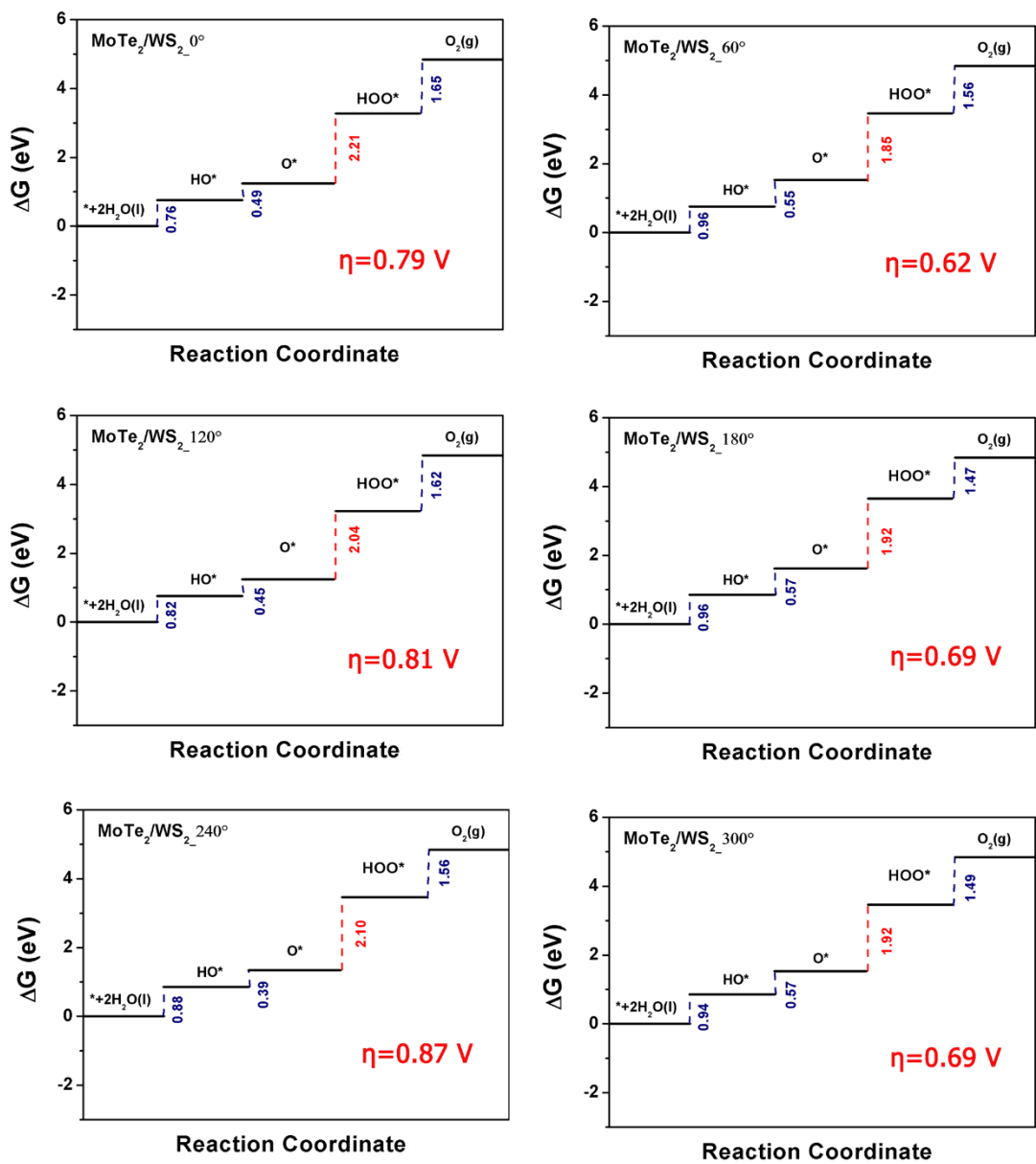


**Figure S9.** Free-energy diagram for OER of MoTe<sub>2</sub>/WS<sub>2</sub> at zero electrode potential.

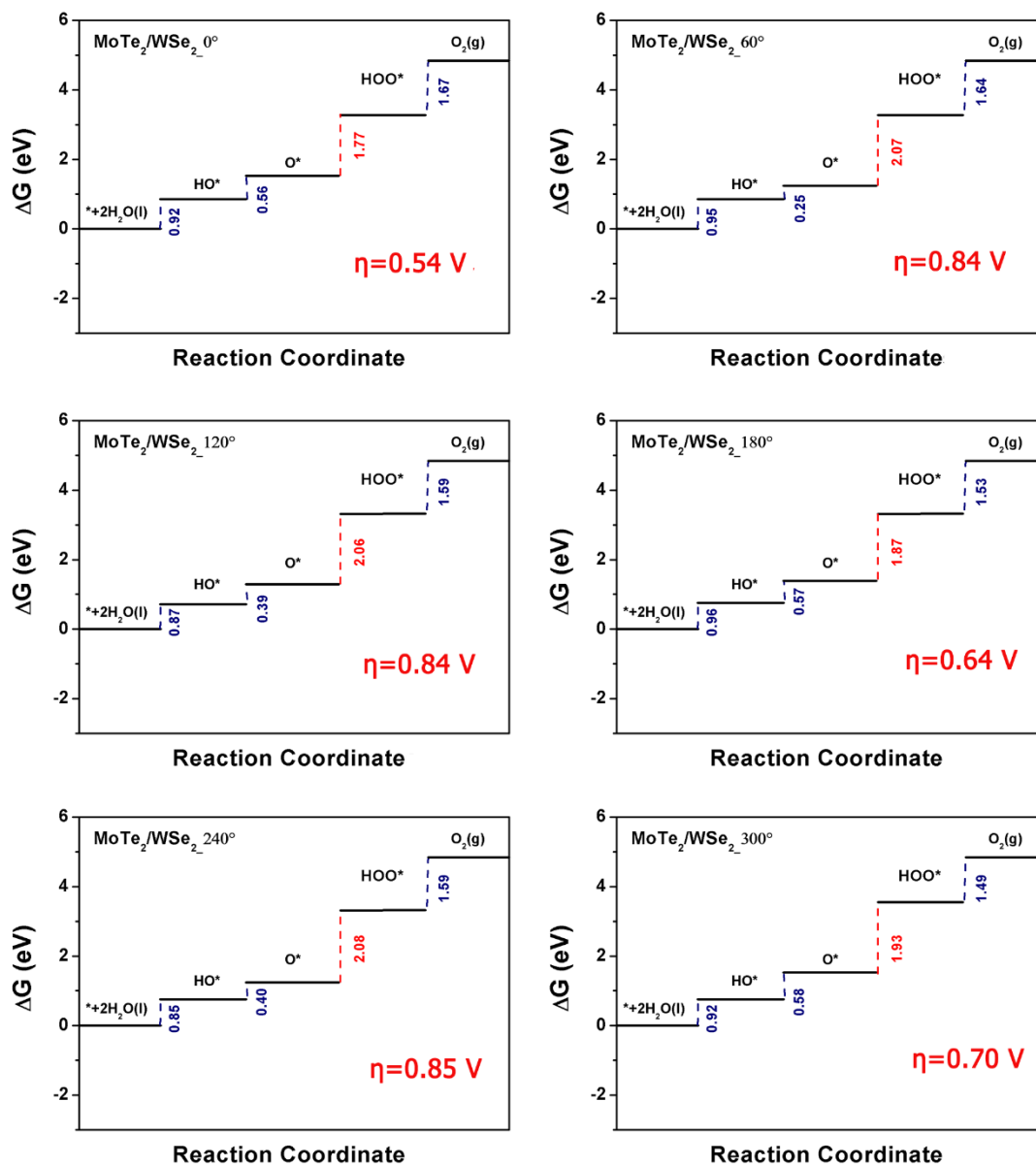


**Figure S10.** Free-energy diagram for OER of MoTe<sub>2</sub>/WSe<sub>2</sub> at zero electrode potential.

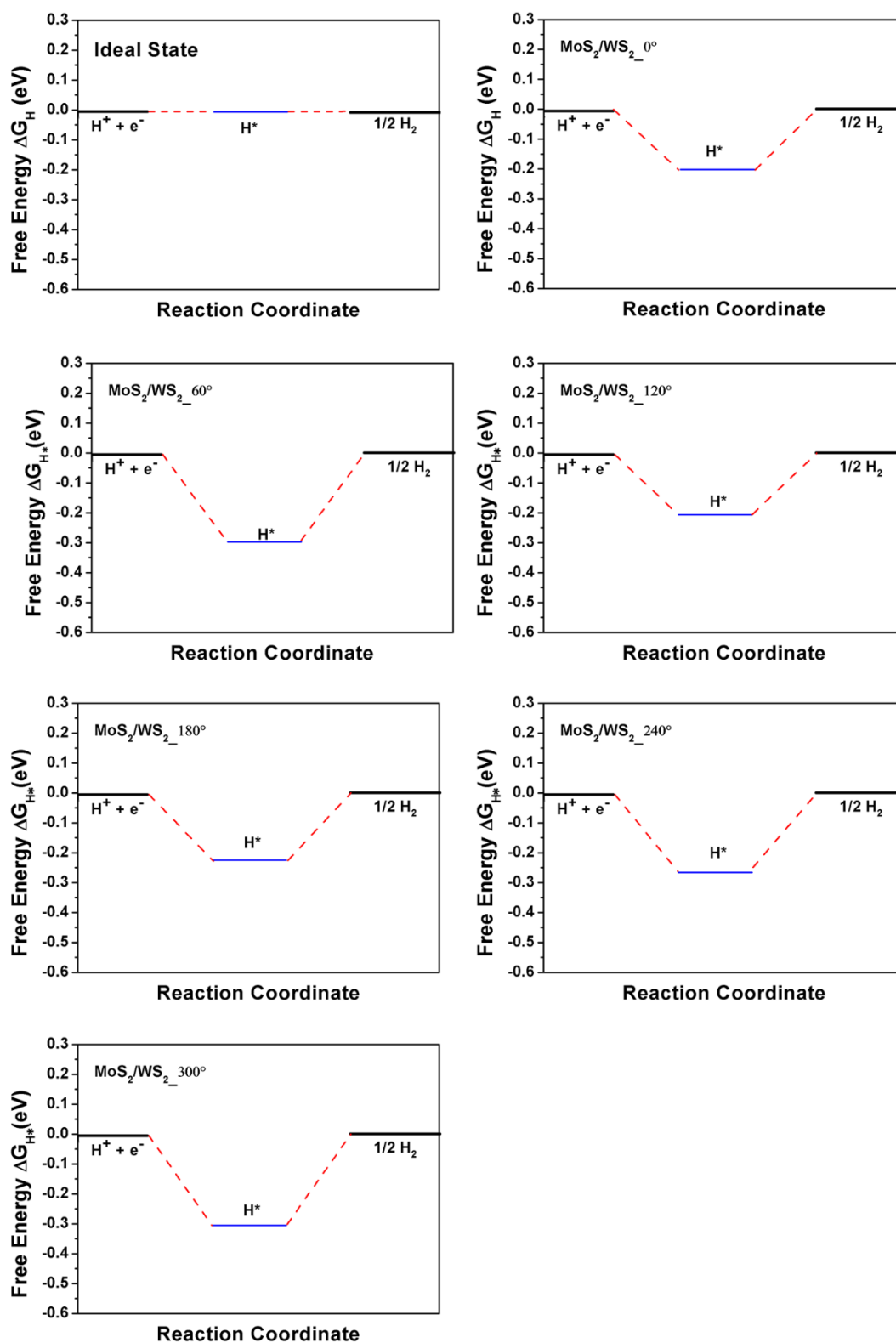


**Figure S11.** Free-energy diagram for HER of MoS<sub>2</sub>/WS<sub>2</sub> at zero electrode potential.

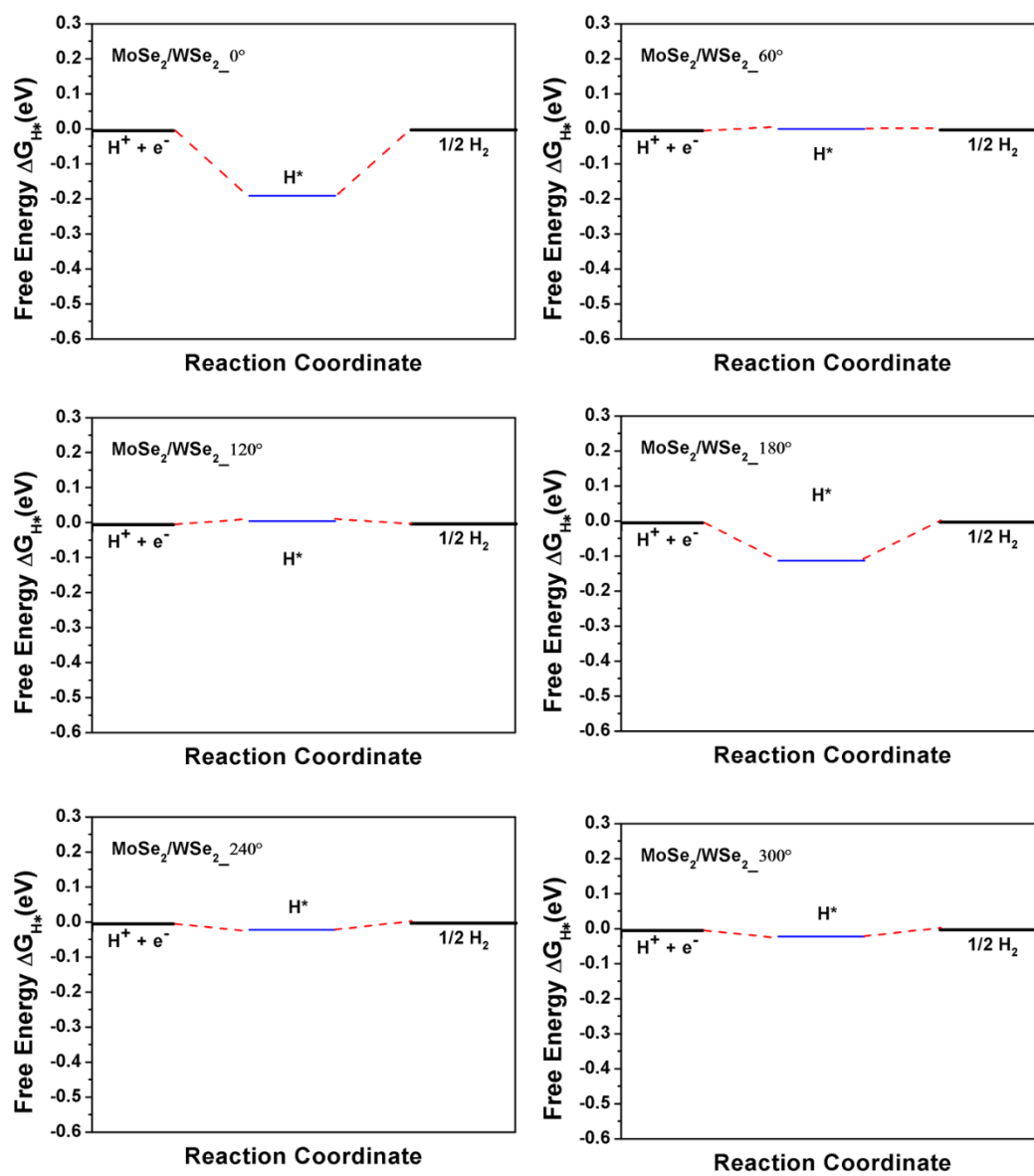


**Figure S12.** Free-energy diagram for HER of MoSe<sub>2</sub>/WSe<sub>2</sub> at zero electrode potential.

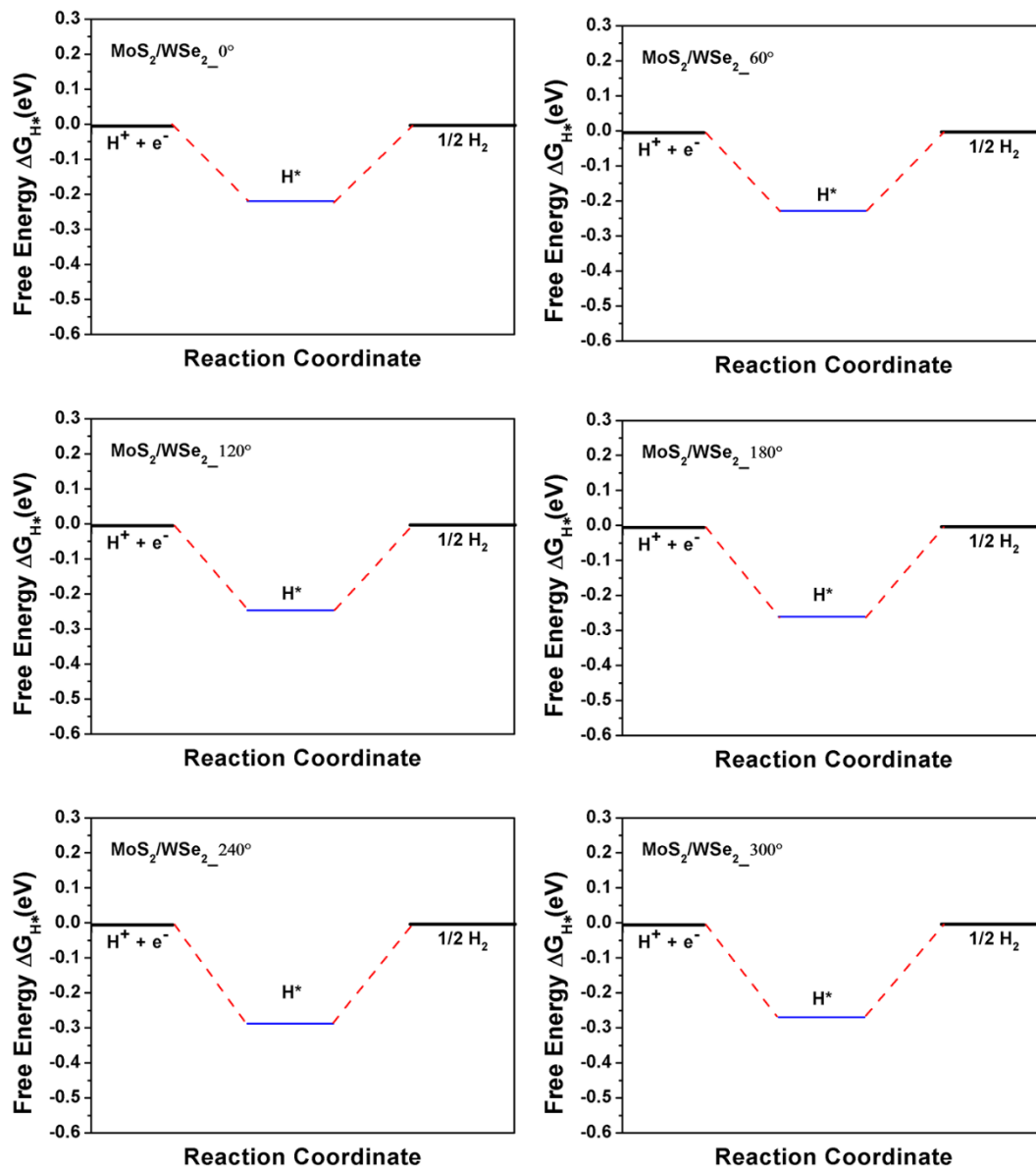


**Figure S13.** Free-energy diagram for HER of MoS<sub>2</sub>/WSe<sub>2</sub> at zero electrode potential.

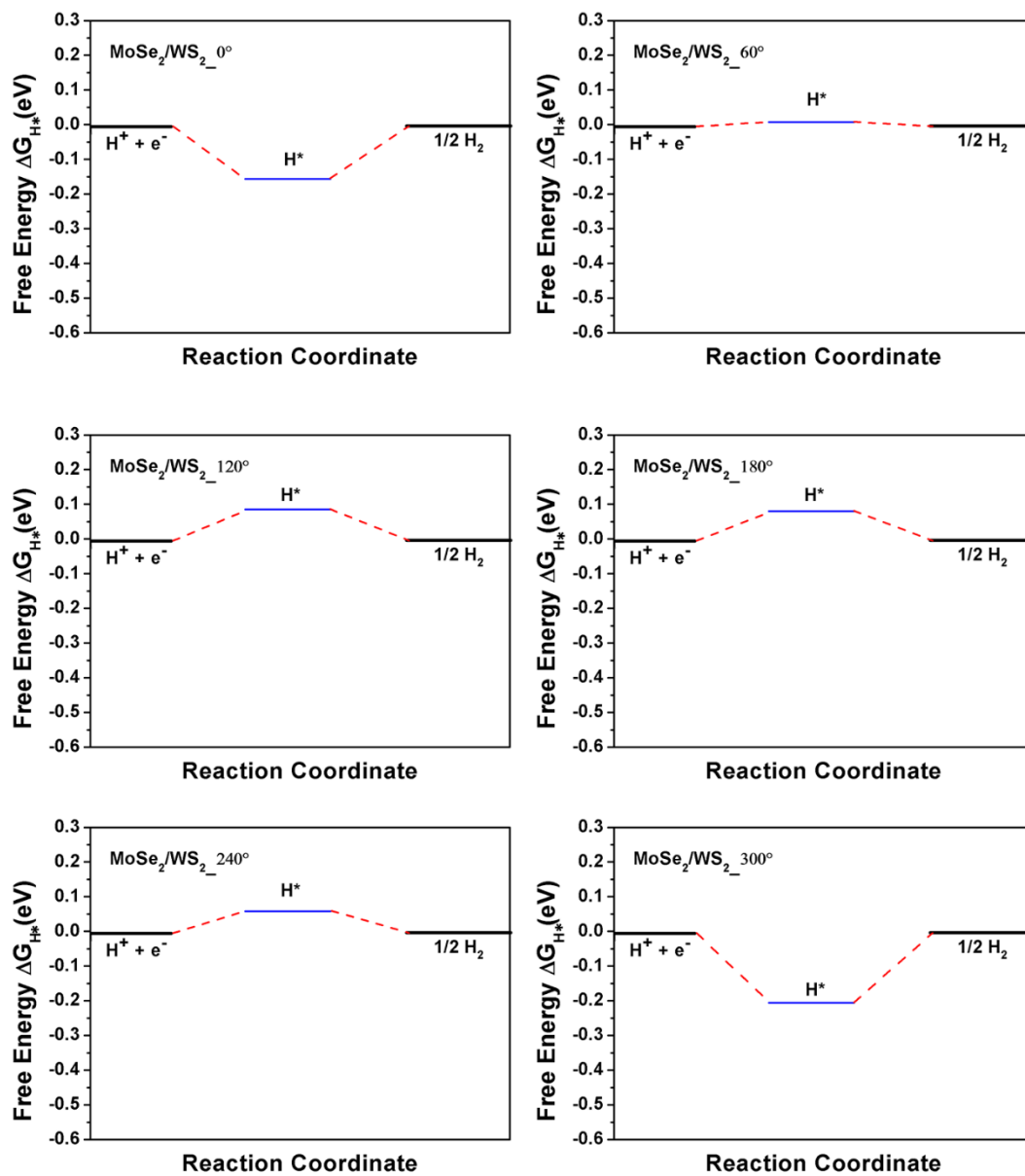


**Figure S14.** Free-energy diagram for HER of MoSe<sub>2</sub>/WS<sub>2</sub> at zero electrode potential.

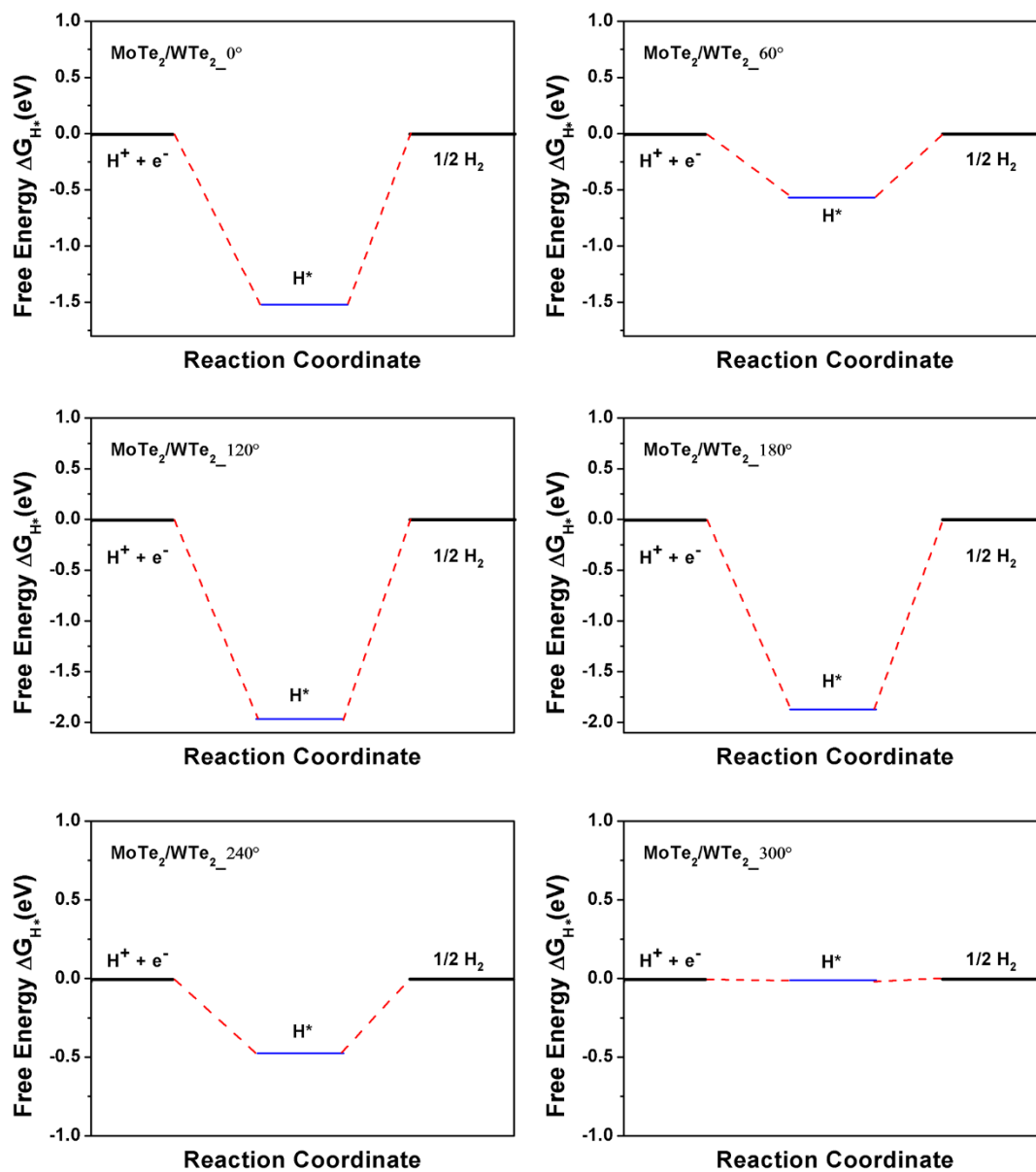


**Figure S15.** Free-energy diagram for HER of MoTe<sub>2</sub>/WTe<sub>2</sub> at zero electrode potential.

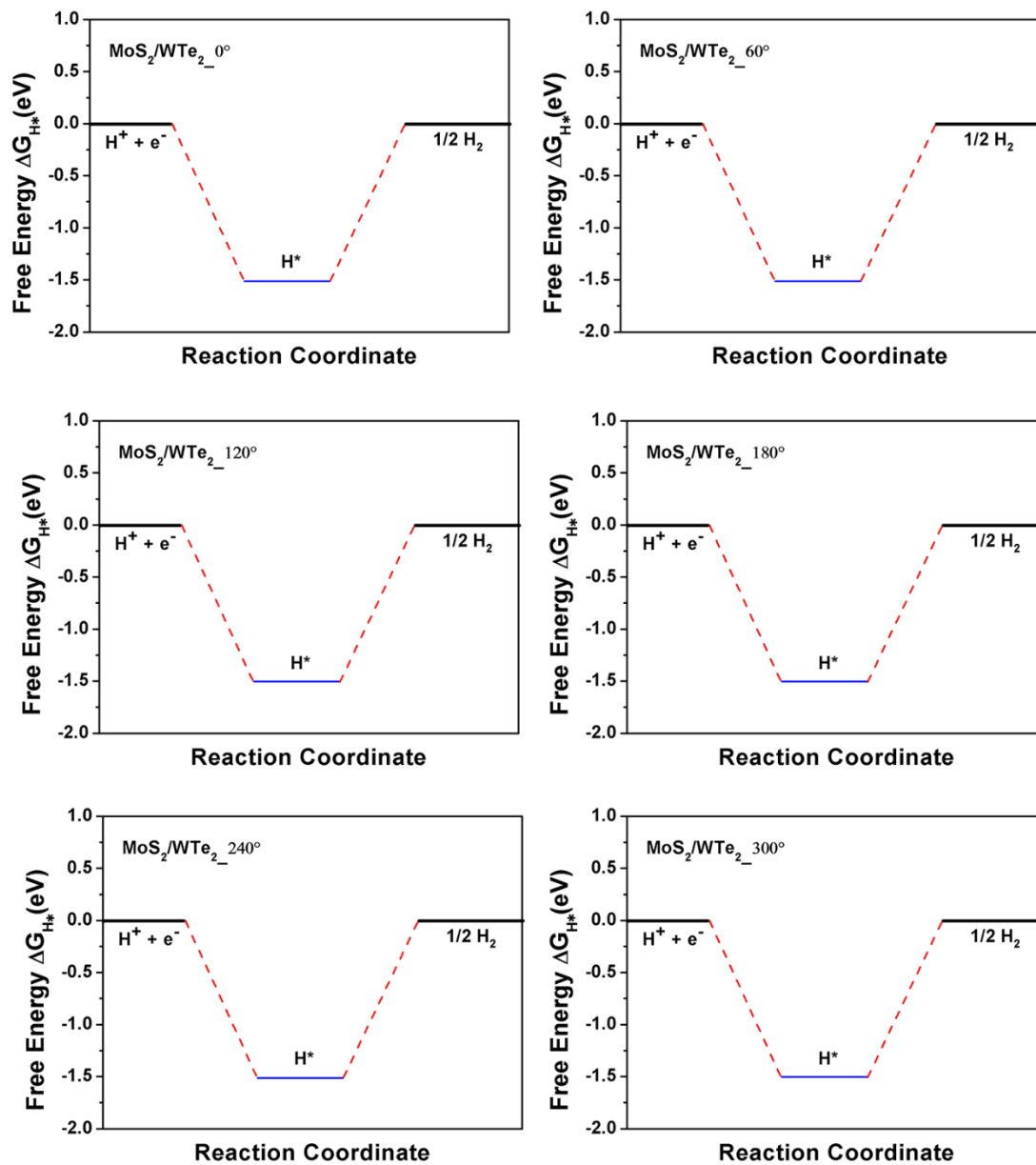


**Figure S16.** Free-energy diagram for HER of MoS<sub>2</sub>/WTe<sub>2</sub> at zero electrode potential.

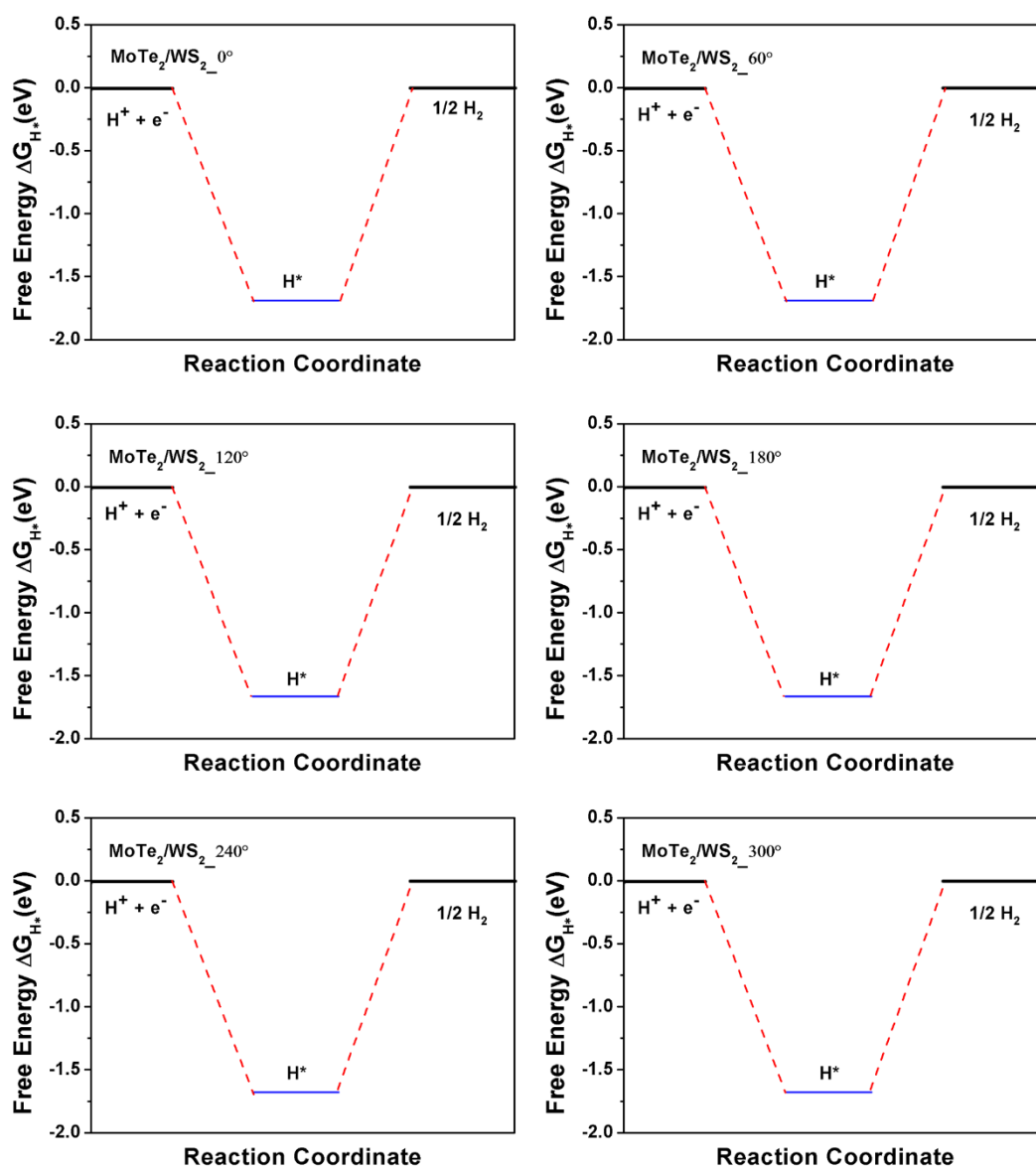


**Figure S17.** Free-energy diagram for HER of MoTe<sub>2</sub>/WS<sub>2</sub> at zero electrode potential.

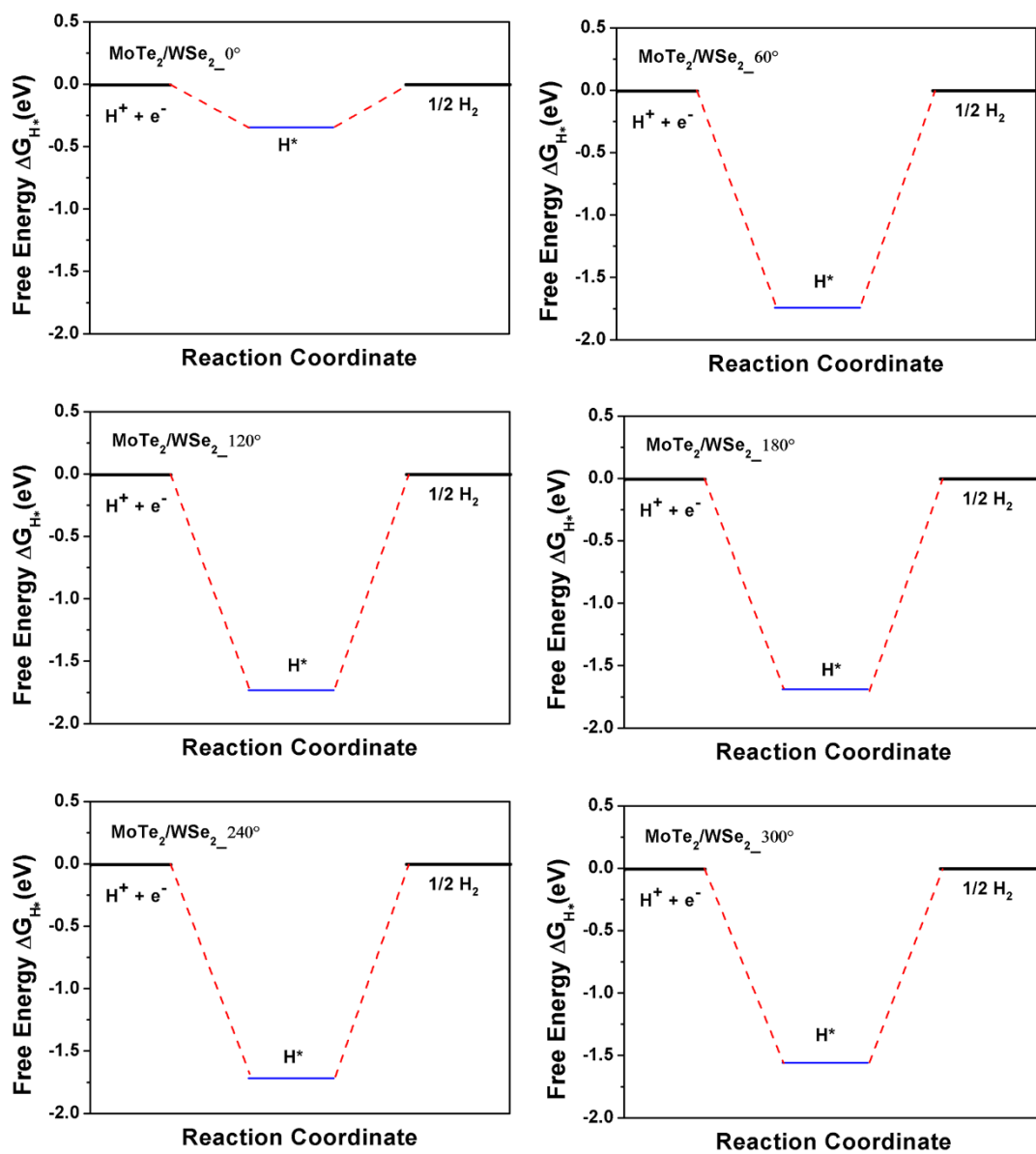


Figure S18. Free-energy diagram for HER of MoTe<sub>2</sub>/WSe<sub>2</sub> at zero electrode potential.

## Supplementary Tables

**Table S1.** The correction for free energy of the gas phase material and adsorbates, including corrections for entropy and enthalpy.

Species	E	TS	E <sub>ZPE</sub>
	(eV)	(eV) (298 K)	(eV)
<b>H<sub>2</sub></b>	-6.86	/	/
<b>H<sub>2</sub>O</b>	-13.71	/	/
<b>H*</b>	/	/	0.205
<b>O*</b>	/	/	0.08
<b>OH*</b>	/	/	0.338
<b>OOH*</b>	/	/	0.398

**Table S2.** The binding energy (eV) of different structures with different rotating angles.

<b>Structure</b>	<b>MoS<sub>2</sub></b>	<b>MoSe<sub>2</sub></b>	<b>MoS<sub>2</sub></b>	<b>MoSe<sub>2</sub></b>	<b>MoTe<sub>2</sub></b>	<b>MoS<sub>2</sub></b>	<b>MoTe<sub>2</sub></b>	<b>MoTe<sub>2</sub></b>
<b>Angle (°)</b>	<b>/WS<sub>2</sub></b>	<b>/WSe<sub>2</sub></b>	<b>/WSe<sub>2</sub></b>	<b>/WS<sub>2</sub></b>	<b>/WT<sub>2</sub></b>	<b>/WTe<sub>2</sub></b>	<b>/WS<sub>2</sub></b>	<b>/WSe<sub>2</sub></b>
	<b>(eV)</b>	<b>(eV)</b>	<b>(eV)</b>	<b>(eV)</b>	<b>(eV)</b>	<b>(eV)</b>	<b>(eV)</b>	<b>(eV)</b>
<b>0</b>	-1.77	-2.29	-2.32	-2.07	-4.41	-2.85	-2.79	-3.01
<b>60</b>	-2.00	-2.49	-2.25	-2.29	-3.41	-2.73	-2.68	-2.90
<b>120</b>	-2.12	-2.59	-2.34	-2.39	-3.52	-2.86	-2.79	-3.02
<b>180</b>	-2.25	-2.74	-2.49	-2.54	-3.78	-3.10	-3.03	-3.26
<b>240</b>	-2.17	-2.66	-2.42	-2.43	-3.60	-2.98	-2.83	-3.09
<b>300</b>	-2.25	-2.66	-2.40	-2.18	-4.46	-3.02	-3.01	-3.22

**Table S3.** Adsorption free energies of \*OH, \*O, \*OOH and \*H (eV) of MoS<sub>2</sub>/ WS<sub>2</sub>.

Angle/ <sup>o</sup>	$\Delta G_{*OH}$ (eV)	$\Delta G_{*O}$ (eV)	$\Delta G_{*OOH}$ (eV)	$\Delta G_{*H}$ (eV)
<b>0</b>	1.67	0.96	3.17	-0.20
<b>60</b>	1.94	1.22	3.80	-0.29
<b>120</b>	2.09	1.32	3.08	-0.22
<b>180</b>	2.08	1.32	3.20	-0.22
<b>240</b>	1.94	1.25	3.23	-0.25
<b>300</b>	2.08	1.31	3.22	-0.30

**Table S4.** Adsorption free energies of \*OH, \*O, \*OOH and \*H (eV) of MoSe<sub>2</sub>/WSe<sub>2</sub>.

Angle/ <sup>o</sup>	$\Delta G_{*OH}$ (eV)	$\Delta G_{*O}$ (eV)	$\Delta G_{*OOH}$ (eV)	$\Delta G_{*H}$ (eV)
<b>0</b>	2.07	1.31	3.09	-0.22
<b>60</b>	1.98	1.31	3.33	-0.23
<b>120</b>	2.00	1.31	4.06	-0.22
<b>180</b>	1.99	1.31	3.75	-0.25
<b>240</b>	1.94	1.30	3.32	-0.26
<b>300</b>	1.94	1.24	3.30	-0.25

**Table S5.** Adsorption free energies of \*OH, \*O, \*OOH and \*H (eV) of MoS<sub>2</sub>/WSe<sub>2</sub>.

Angle/°	$\Delta G_{*OH}$ (eV)	$\Delta G_{*O}$ (eV)	$\Delta G_{*OOH}$ (eV)	$\Delta G_{*H}$ (eV)
<b>0</b>	1.47	1.91	3.83	-0.15
<b>60</b>	2.04	2.23	4.03	0.09
<b>120</b>	1.93	2.24	3.98	0.10
<b>180</b>	1.91	2.24	4.07	0.09
<b>240</b>	1.87	2.23	4.01	0.07
<b>300</b>	1.63	1.86	3.61	-0.19

**Table S6.** Adsorption free energies of \*OH, \*O, \*OOH and \*H (eV) of MoSe<sub>2</sub>/WS<sub>2</sub>.

Angle/°	$\Delta G_{*OH}$ (eV)	$\Delta G_{*O}$ (eV)	$\Delta G_{*OOH}$ (eV)	$\Delta G_{*H}$ (eV)
<b>0</b>	1.62	1.93	3.68	-0.17
<b>60</b>	1.90	2.23	4.55	0.10
<b>120</b>	2.03	2.23	4.81	0.10
<b>180</b>	1.95	2.21	3.95	-0.11
<b>240</b>	2.43	2.22	3.98	-0.01
<b>300</b>	1.80	2.12	3.91	-0.03

**Table S7.** Adsorption free energies of \*OH, \*O, \*OOH and \*H (eV) of MoTe<sub>2</sub>/WTe<sub>2</sub>.

Angle/ <sup>o</sup>	$\Delta G_{*OH}$ (eV)	$\Delta G_{*O}$ (eV)	$\Delta G_{*OOH}$ (eV)	$\Delta G_{*H}$ (eV)
<b>0</b>	1.12	2.18	3.53	-1.54
<b>60</b>	0.15	0.95	2.45	0.58
<b>120</b>	0.29	0.68	2.65	-1.97
<b>180</b>	0.92	1.48	2.81	-1.89
<b>240</b>	0.34	1.22	2.70	-0.48
<b>300</b>	1.08	2.15	3.51	-0.03

**Table S8.** Adsorption free energies of \*OH, \*O, \*OOH and \*H (eV) of MoS<sub>2</sub>/WTe<sub>2</sub>.

Angle/ <sup>o</sup>	$\Delta G_{*OH}$ (eV)	$\Delta G_{*O}$ (eV)	$\Delta G_{*OOH}$ (eV)	$\Delta G_{*H}$ (eV)
<b>0</b>	1.77	1.22	2.19	-1.52
<b>60</b>	1.92	1.26	2.45	-1.52
<b>120</b>	1.54	1.26	2.02	-1.51
<b>180</b>	1.82	1.26	2.24	-1.51
<b>240</b>	1.80	1.25	3.98	-1.52
<b>300</b>	1.80	1.26	2.24	-1.51

**Table S9.** Adsorption free energies of \*OH, \*O, \*OOH and \*H (eV) of MoTe<sub>2</sub>/WS<sub>2</sub>.

Angle/ <sup>o</sup>	$\Delta G_{*OH}$ (eV)	$\Delta G_{*O}$ (eV)	$\Delta G_{*OOH}$ (eV)	$\Delta G_{*H}$ (eV)
<b>0</b>	0.76	1.25	3.27	-1.71
<b>60</b>	0.96	1.51	3.36	-1.71
<b>120</b>	0.82	1.27	3.30	-1.70
<b>180</b>	0.96	1.53	3.45	-1.66
<b>240</b>	0.88	1.26	3.36	-1.70
<b>300</b>	0.94	1.51	3.43	-1.67

**Table S10.** Adsorption free energies of \*OH, \*O, \*OOH and \*H (eV) of MoTe<sub>2</sub>/WSe<sub>2</sub>.

Angle/ <sup>o</sup>	$\Delta G_{\text{OH}^*}$ (eV)	$\Delta G_{\text{O}^*}$ (eV)	$\Delta G_{\text{OOH}^*}$ (eV)	$\Delta G_{\text{H}^*}$ (eV)
<b>0</b>	0.92	1.48	3.25	-0.34
<b>60</b>	0.95	1.20	3.28	-1.72
<b>120</b>	0.87	1.26	3.33	-1.71
<b>180</b>	0.96	1.52	3.39	-1.68
<b>240</b>	0.85	1.25	3.33	-1.71
<b>300</b>	0.92	1.50	3.43	-1.54

## Supplementary References

- (1) Kramm, U. I.; Herrmann-Geppert, I.; Behrends, J.; Lips, K.; Fiechter, S.; Bogdanoff, P. On an Easy Way To Prepare Metal–Nitrogen Doped Carbon with Exclusive Presence of MeN<sub>4</sub>-Type Sites Active for the ORR. *J. Am. Chem. Soc.* **2016**, *138*, 635–640.
- (2) Ling, C.; Shi, L.; Ouyang, Y.; Zeng, X. C.; Wang, J. Nanosheet Supported Single-Metal Atom Bifunctional Catalyst for Overall Water Splitting. *Nano Lett.* **2017**, *17*, 5133–5139.
- (3) Costentin, C.; Savéant, J.-M. Towards an Intelligent Design of Molecular Electrocatalysts. *Nat. Rev. Chem.* **2017**, *1*, 1–8.
- (4) Zitolo, A.; Goellner, V.; Armel, V.; Sougrati, M.-T.; Mineva, T.; Stievano, L.; Fonda, E.; Jaouen, F. Identification of Catalytic Sites for Oxygen Reduction in Iron- and Nitrogen-Doped Graphene Materials. *Nat. Mater.* **2015**, *14*, 937–942.
- (5) Liu, W.; Zhang, L.; Yan, W.; Liu, X.; Yang, X.; Miao, S.; Wang, W.; Wang, A.; Zhang, T. Single-Atom Dispersed Co–N–C Catalyst: Structure Identification and Performance for Hydrogenative Coupling of Nitroarenes. *Chem. Sci.* **2016**, *7*, 5758–5764.
- (6) Man, I. C.; Su, H.-Y.; Calle-Vallejo, F.; Hansen, H. A.; Martínez, J. I.; Inoglu, N. G.; Kitchin, J.; Jaramillo, T. F.; Nørskov, J. K.; Rossmeisl, J. Universality in Oxygen Evolution Electrocatalysis on Oxide Surfaces. *ChemCatChem* **2011**, *3*, 1159–1165.